jmb

Production of D-Xylonic Acid from Hemicellulose Using Artificial Enzyme Complexes

Charles C. Lee[1*], Rena E. Kibblewhite[1], Chad D. Paavola[2], William J. Orts[1], and Kurt Wagschal[1]

[1]USDA-ARS-WRRC, Bioproducts Research Unit, Albany, CA 94710, USA

[2]NASA Ames Research Center, Moffett Field, CA 94035, USA

Lignocellulosic biomass represents a potentially large resource to supply the world's fuel and chemical feedstocks. Enzymatic bioconversion of this substrate offers a reliable strategy for accessing this material under mild reaction conditions. Owing to the complex nature of lignocellulose, many different enzymatic activities are required to function in concert to perform efficient transformation. In nature, large multienzyme complexes are known to effectively hydrolyze lignocellulose into constituent monomeric sugars. We created artificial complexes of enzymes, called rosettazymes, in order to hydrolyze glucuronoxylan, a common lignocellulose component, into its cognate sugar D-xylose and then further convert the D-xylose into D-xylonic acid, a Department of Energy top-30 platform chemical. Four different types of enzymes (endoxylanase, α-glucuronidase, β-xylosidase, and xylose dehydrogenase) were incorporated into the artificial complexes. We demonstrated that tethering our enzymes in a complex resulted in significantly more activity (up to 71%) than the same amount of enzymes free in solution. We also determined that varying the enzyme composition affected the level of complex-related activity enhancement as well as overall yield.

Keywords: Lignocellulose, multienzyme assembly, bioconversion, glucuronoxylan, xylonic acid

Introduction

The world's continued reliance on fossil fuels to supply our chemical feedstock and fuel needs is unsustainable owing to environmental damage from extraction, climate change from combustion, and eventual resource depletion. It is estimated that there are greater than 220 billion tons of lignocellulosic biomass available globally, which represents a tremendous renewable source for society's chemical demands [1, 2]. Furthermore, the use of this waste biomass avoids conflicts that arise from the "food vs fuel" debate [3]. However, the difficulty and costs associated with processing the lignocellulose make the transition from fossil fuels to this renewable resource very challenging [1, 4, 5]. Therefore, much attention has been placed on efficiently deriving value-added byproducts from all fractions of biomass.

The main component of biomass is cellulose, which is a polymer of β-1,4-linked glucose residues that can be hydrolyzed to simple sugars by three classes of enzymes and then relatively easily fermented to ethanol or other chemicals [6, 7]. The second most common fraction of biomass is hemicellulose. Glucuronoxylan is one type of hemicellulose, and it is a polymer of β-1,4-linked xylose residues [8]. The structure of glucuronoxylan is more complex than cellulose. Different chemical moieties branch off the polymer, and these decorations inhibit the action of the main chain-degrading enzymes in hydrolyzing the polymer to simple sugars [9, 10]. For instance, one of the most common decorations is glucuronic acid and its 4-0-methyl derivative, collectively referred to as (4Me)-GlcA, which form an α-1,2-linkage with the xylose residue. (4Me)-GlcA can decorate more than 18% of the residues on the glucuronoxylan polymer, and the presence of this moiety prevents the complete breakdown of glucuronoxylan into monomeric xylose. A specific accessory enzyme is required for the removal of each type of chemical decoration [10]. Thus, the presence of these branched structures necessitates a wider variety of enzyme classes to fully hydrolyze this

hemicellulose polymer into xylose [11]. Much research has been focused on the isolation and engineering of these various enzymes to facilitate greater hydrolysis efficiencies [12−15].

While xylose can be fermented into ethanol, the sugar can also be oxidized to xylonic acid. Xylonic acid was identified as one of the top-30 platform chemicals from which to support a biobased economy [16]. This multipurpose chemical has a variety of potential uses, including as a concrete dispersal agent and a building block of copolyamide polymers [17, 18]. Furthermore, it has been utilized as a precursor for other chemicals, such as 1,2,4-butanetriol, which is also a valuable feedstock chemical involved in the synthesis of plasticizers, polymers, and medical precursors for drug delivery [19, 20].

One of the most efficient enzymatic strategies for hydrolyzing biomass substrates is the use of multienzyme complexes called cellulosomes, produced by various anaerobic bacteria [21, 22]. These complexes are composed of a protein scaffold containing multiple recognition sites called cohesins. Biomass-degrading enzymes with complementary recognition motifs called dockerins will bind to the cohesins to form large complexes that are very effective at hydrolyzing cellulosic biomass. The composition of enzymes that bind to the scaffold fluctuates depending on the carbon source fed to the bacteria [23].

There is great interest in creating designer cellulosomes not only to efficiently hydrolyze different biomass substrates, but also to understand the dynamics of enhanced bioconversion. Due in part to the difficulty of working with the large native scaffold protein (197 kD), many studies have created artificial mini-scaffolds that contain two to six cohesin domains [24−28]. These scaffolds can be stacked to create structures with even greater numbers of cohesin domains (up to 12) to bind enzymes [29, 30]. Using such systems, it has been clearly demonstrated that enzymes tethered to the scaffold show much more activity to hydrolyze biomass substrates than the same enzymes free in solution. This complex-induced enhancement is due in part to the phenomenon of "substrate channeling," whereby concentrations of intermediates are increased as a result of the colocalization of enzymes that are part of the same pathway [31].

We were interested in creating larger multienzyme complexes to facilitate biotransformations in which biomass is hydrolyzed and further chemically transformed to value-added product. We used a chaperonin protein from the thermophilic *Sulfolobus shibatae* bacterium that was engineered to contain a cohesin site [32, 33]. Eighteen subunits of this protein self-assemble into a double-ring scaffold with nine enzyme binding sites on each face of the structure [33−36]. In this report, we demonstrate the use of this artificial scaffold in enhancing production of xylonic acid from a glucuronoxylan substrate.

Materials and Methods

Reagents and Cell Lines

Escherichia coli BL21 (DE3) pLysE and BL21 CodonPlus (DE3)-RIPL cells were obtained from ThermoFisher Scientifics (USA) and Agilent Technologies (USA), respectively. pET-22b(+) and pET-29b(+) expression plasmids were obtained from EMD Millipore (USA). All other chemicals and reagents were obtained from Sigma Aldrich (USA) unless otherwise specified.

Expression Vectors

The rosettasome-cohesin (RC) scaffold subunit gene was cloned into the pET19b vector as described previously [32]. The dockerin domain from the *celF* gene (GenBank X60545.1) [37] was fused to the C-termini of the genes encoding xylanase (*Y2-xyn10*; GenBank DQ059337), α-glucuronidase (*Rum63ag*; GenBank JN684207), β-xylosidase (*SXA*; GenBank AF040720), and xylose dehydrogenase (*xylB*; GenBank CP001340.1). The *celF*-dockerin gene fragment was isolated by PCR amplification using the following primers:

docL-5f: GTACCTCGAGGGAGGTTCGGAGCCCGAT
doc-S-3f: GCAGCGGCCGCCTGTTCAGCCGGGAATTTTTCA

The PCR product was then digested with the XhoI and NotI restriction enzymes. The *xylB* gene was synthesized (Genscript, USA) whereas the other three genes (*Y2-xyn10*, *Rum630ag*, and *SXA*) were present in plasmids from our collection. The genes encoding these four enzymes were subjected to restriction enzyme digestion to create NdeI and XhoI compatible sites at the 5' and 3' ends of the genes, respectively. The DNA encoding the *Y2-xyn10* gene and the *celF*-dockerin PCR fragment were subcloned into the NdeI/NotI-digested pET-22b(+) vector. The DNAs encoding the remaining three genes (*xylB*, *Rum630ag*, and *SXA*) were each combined with the *celF*-dockerin PCR fragment and were subcloned into the NdeI/NotI-digested pET-29b(+) vector. The resulting genes all contained a C-terminal six-histidine tag.

Protein Expression and Purification

The RC expression vector was transformed into the BL21 CodonPlus (DE3)-RIPL cell line and expressed and purified as previously described [32]. The *SXA*-dockerin expression vector was transformed into BL21 (DE3) pLysE, whereas the remaining enzyme-dockerin vectors were transformed into BL21 CodonPlus (DE3)-RIPL.

The *SXA*-dockerin and *xylB*-dockerin cell lines were grown in Luria Bertani broth at 30°C until they reached an optical density at 600 nm of 0.7. Isopropyl β-D-1-thiogalactopyranoside was added to a final concentration of 1 mM, and cells were harvested by

centrifugation after 3 h. The Y2-Xyn10 and Rum630AG cell lines were grown at 37°C in auto-induction media (ZYM-5052) for 24 h and then harvested by centrifugation [38]. All cell lines were grown in the presence of the appropriate antibiotic: ampicillin or kanamycin for the pET22b(+)- or pET29b(+)-derived plasmids, respectively.

The *SXA*-dockerin and *XylB*-dockerin cell pellets were lysed by the addition of CelLytic (Sigma Aldrich, USA) supplemented with protease inhibitor cocktail (EMD Millipore, USA), benzonase (EMD Millipore, USA), hen egg white lysozyme, and PMSF. Y2-Xyn10 and Rum630AG cell pellets were lysed by resuspension in 50 mM sodium phosphate, benzonase, hen egg white lysozyme, and protease inhibitor cocktail. All the resuspended cells were subjected to additional sonication followed by centrifugation.

The soluble protein fraction was supplemented with imidazole (10 mM) and sodium chloride (300 mM) and then applied to nickel Sepharose columns (EMD Millipore, USA). The enzymes were eluted by an imidazole gradient in 50 mM sodium phosphate buffer, pH 7.2. The fractions containing purified enzymes were pooled, and the buffer was exchanged over a 10G Econopac column (Biorad, USA) containing 50 mM sodium phosphate, 50 mM sodium chloride, and 10% glycerol, pH 7.2.

Biochemical Characterization of Enzymes

Each enzyme-dockerin fusion was individually characterized using the appropriate substrate at various concentrations. Xylanase, α-glucuronidase, β-xylosidase, and xylose dehydrogenase were assayed against birchwood xylan, aldouronic acid (Megazyme, Ireland), xylobiose, and xylose, respectively. All reactions were conducted at 25°C in 40 mM MES buffer (pH 6.5) and measured on a plate reader (spectramax M; Molecular Devices, USA). Xylanase reaction products were detected by adding DNSA solution (1% dinitrosalicyclic acid and 30% potassium sodium tartrate in 0.5 M sodium hydroxide), heating the samples at 100°C for 5 min, and measuring the optical density at 562 nm as previously described [39]. α-Glucuronidase reaction products were measured using a protocol of Milner and Avigad [40] by adding copper solution A, heating at 100°C for 15 min, adding arsenomolybdate reagent B, and measuring at 750 nm. β-Xylosidase products were detected using an enzyme-linked assay that utilized pyranose oxidase, horseradish peroxidase, and the chromogen 2,2′-azino-*bis*(3-ethylbenzothiazoline-6-sulfonate) followed by measuring at 420 nm as previously described [41]. Xylose dehydrogenase product formation was measured by monitoring the concomitant reduction of NAD$^+$ to NADH as measured at 340 nm [42].

Rosettazyme Assembly

RC subunits at a concentration of 14.9 μM were incubated overnight at 4°C in the presence of 25 mM MgCl$_2$ and 1 mM ATP in order to assemble the double-ring scaffold. The next day, the rosettazymes were formed by incubating a solution of 1 μM scaffold with 1 μM total enzyme in 5 mM CaCl$_2$ and 40 mM MES buffer, pH 6.5, at 21°C for 30 min. Various ratios of enzymes were loaded onto the scaffold, but the total enzyme concentration was maintained at 1 μM. Corresponding enzyme mixtures containing no scaffold (termed "free") were prepared in similar fashion, except that 1 mM ATP and 25 mM MgCl$_2$ were used in place of the RC double-ring scaffold.

Xylonic Acid Formation Activity Assays

Rosettazyme enzyme complexes (50 nM) were incubated with 1% birchwood substrate (Sigma Aldrich, USA), 4 mM NAD$^+$, 2.5 mM MgCl$_2$, and 40 mM MES, pH 6.5. The reactions were carried out in duplicates at 25°C and monitored periodically for 3 h. The formation of xylonic acid was measured by the reduction of NAD$^+$ to NADH with a concurrent increase in absorption at 340 nm (Spectramax M2 plate reader).

Results and Discussion

Three enzymes necessary to fully hydrolyze glucuronoxylan into monomeric xylose sugars are xylanase (E.C. 3.2.1.8), α-glucuronidase (E.C. 3.2.1.139), and β-xylosidase (E.C. 3.2.1.37) (Fig. 1). A glycosyl hydrolase family 10 (GH10) xylanase (Xyn, [43]) was chosen for this study because this
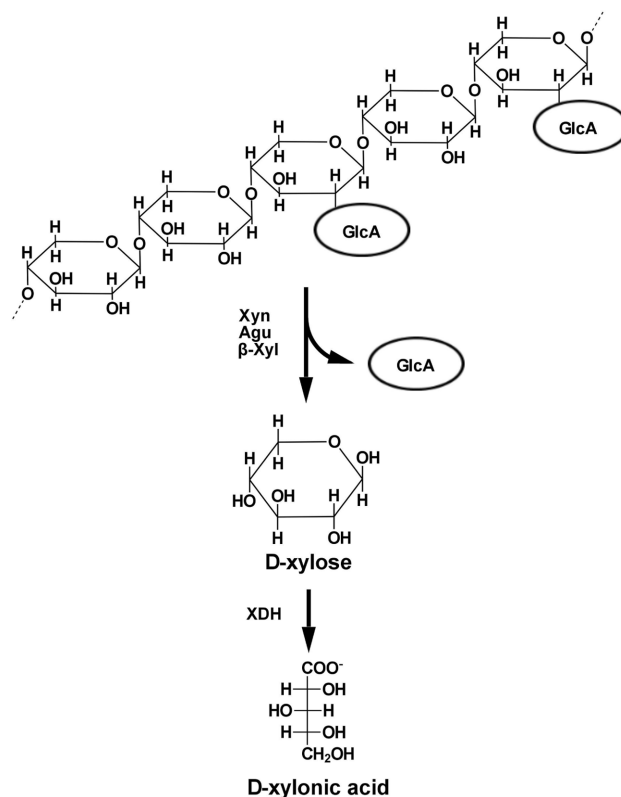

Fig. 1. Enzymatic conversion of branched glucuronoxylan substrate to xylonic acid.

Xyn, xylanase; Agu, α-glucuronidase; β-Xyl, β-xylosidase; XDH, xylose dehydrogenase; GlcA, (4Me)-glucuronic acid branch.

category of xylanase is known to accept branched glucuronoxylan as a substrate. These xylanases cleave the substrate to produce short xylooligosaccharides that are substituted at the non-reducing end with a (4Me)-glucuronic acid moiety [44]. A GH67 α-glucuronidase (Agu) enzyme was used because this enzyme has been demonstrated to remove (4Me)-glucuronic acid from these xylooligosaccharide fragments [45]. Our previous work with these two specific enzymes had demonstrated that they act synergistically to release the (4Me)-glucuronic acid moiety from the substrate. To hydrolyze the debranched xylooligosaccharide into monomeric xylose, the *Selenomonas ruminantium* β-xylosidase (β-Xyl) enzyme was used. This enzyme had been previously demonstrated to have high activity against xylooligosaccharides [46]. The final step in the bioconversion of xylose to xylonic acid was mediated by the xylose dehydrogenase enzyme (XDH) from *Caulobacter crescentus* [47]. This enzyme had been successfully heterologously expressed by multiple groups for in vivo xylose bioconversion [20, 48, 49].

The genes for all four enzymes were fused to a naturally occurring dockerin motif from *Clostridium thermocellum* (Fig. 2A). The enzymes could then be bound to the double-ring scaffold, which encoded the complementary cohesin binding sites to form the rosettazyme complex (Fig. 2B). For each bioconversion reaction, 50 nM of total enzyme in e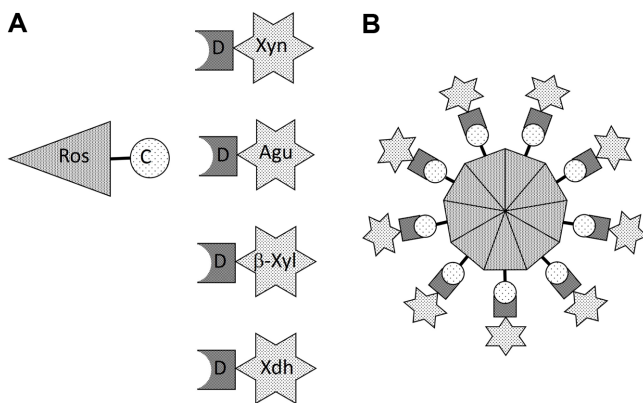quimolar ratio (12.5 nM each enzyme) was incubated with the glucuronoxylan substrate. The rossettazyme enzyme complexes produced more xylonic acid than the equivalent amount of enzyme free in solution (Fig. 3). At each time point measured from 60 to 180 min, there was approximately 35% enhancement in xylonic acid produced by the rosettazyme compared with the same amount of enzyme free in solution.

To determine the effect of different enzyme ratios on the levels and complex enhancement of xylonic acid production, the relative amounts of each of the enzymes were varied while still maintaining 50 nM total enzyme (Fig. 4). When equimolar concentrations of enzymes were used, 152.4 ± 12.4 μM xylonic acid was produced. When Xyn and XDH were used at the lowest concentrations, the amount of product was significantly decreased (reactions 2, 3, and 4). However, increasing the amount of XDH could largely compensate for this decreased production (reactions 5, 6, and 7). Similarly, increasing the amount of Xyn could also partially compensate for the lower levels of XDH (reactions 8, 9, and 11). The levels of the Agu and β-Xyl enzymes did not seem to have as much of an impact in those reactions. Further exemplifying the role of Xyn and XDH, reaction 10, with the highest level of both these enzymes combined, also resulted in the greatest amount of product produced (286.7 ± 0.2 μM). The need for higher levels of Xyn enzyme (k_{cat} = 117 s^{-1}) is likely due in part to the enzyme's role in the first step of the bioconversion pathway. A lower concentration of the β-Xyl enzyme may be required because this particular enzyme has a very high specific activity (k_{cat} = 330 s^{-1}). On

Fig. 2. Rosettazyme complex assembly.
(**A**) Schematic of rosettazyme-cohesin (RC) subunit and individual enzyme-dockerin fusions. (**B**) Fully assembled double-ring rosettazyme complexed with various enzymes. This top view shows only nine of the 18 subunits. The other nine subunits are located beneath this top layer. Ros-C, rosettazyme-cohesin (RC) subunit; D, dockerin domain fused to various enzymes. All other abbreviations are the same as described in Fig. 1.
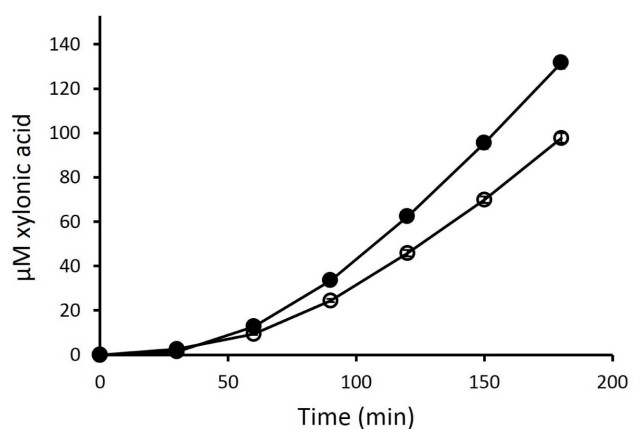

Fig. 3. Xylonic acid production.
The hydrolysis of glucuronoxylan substrate and subsequent conversion of xylose sugar to xylonic acid by 50 nM enzymes free in solution (open circles) and enzymes complexed in the rosettazymes (filled circles). Error bars are approximately the size of the symbols.
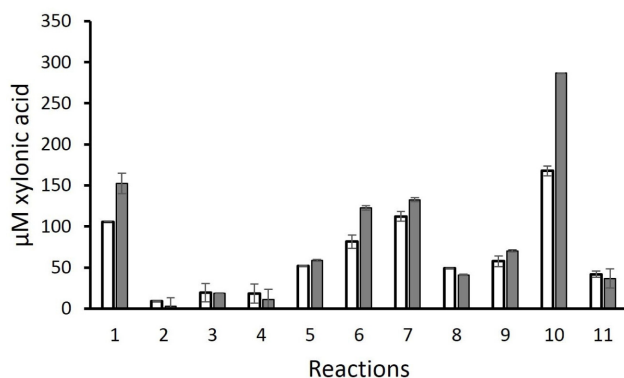
Various ratios of enzymes				
Reaction	**Xyn**	**Agu**	**β-Xyl**	**XDH**
#1	2.5	2.5	2.5	2.5
#2	1	7	1	1
#3	1	4	4	1
#4	1	1	7	1
#5	1	4	1	4
#6	1	1	4	4
#7	1	1	1	7
#8	4	4	1	1
#9	4	1	4	1
#10	4	1	1	4
#11	7	1	1	1

Fig. 4. Effects of various enzyme ratios on xylonic acid production.
A total enzyme concentration of 50 nM was used in each reaction, while the relative amounts of each of four proteins was varied. Production from enzymes deployed free in solution (open bars) was compared with those complexed in the rosettazyme (filled bars) at 180 min. All abbreviations are the same as described in Fig. 1.

the other hand, only a low concentration of the Agu enzyme was required despite the fact that it has a lower specific activity ($k_{cat} = 31$ s^{-1}). This could be explained by the recognition that there are many fewer (4Me)-glucuronic acid moieties to release compared with the number of xylosidic bonds. Finally, the need for higher levels of the XDH enzyme is explained by the enzyme's lower specific activity ($k_{cat} = 7.6$ s^{-1}).

The production enhancement observed with the complex formation at equimolar ratio (reaction 1) was not uniformly observed with all of the other ratios. For instance, most of the reactions (2, 3, 4, 5, 8, 9, and 11) did not show significant levels of enhancement. Modest enhancement was seen in reactions 6 and 7, which had higher levels of XDH. The reaction with the greatest level of enhancement (71%) was reaction 10, which had higher concentrations of both Xyn and XDH. Thus, it is clear that the production enhancement observed when enzymes are deployed as a rosettazyme complex (vs free in solution) is not observed in most instances even when the same types of enzymes are utilized. This result indicates that simply colocalizing enzymes onto a scaffold is insufficient to ensure production enhancement. This may be due to the levels of intermediates that are produced along the biosynthetic pathway. Unless optimal local concentrations of intermediates are produced at each step, a balanced overall flux might not be maintained, and colocalized enzymes may be unable to maximally benefit from their close proximity. This highlights the need to empirically determine any enhancement effect from complexing enzymes onto such a scaffold for each enzyme mixture.

References

1. Ren N, Wang A, Cao G, Xu J, Gao L. 2009. Bioconversion of lignocellulosic biomass to hydrogen: potential and challenges. *Biotechnol. Adv.* **27:** 1051-1060.

2. Kircher M. 2015. Sustainability of biofuels and renewable chemicals production from biomass. *Curr. Opin. Chem. Biol.* **29:** 26-31.

3. Tyner WE. 2013. Biofuels and food prices: separating wheat from chaff. *Glob. Food Sec.* **2:** 126-130.

4. Balan V. 2014. Current challenges in commercially producing biofuels from lignocellulosic biomass. *ISRN Biotechnol.* **2014:** 463074.

5. McCann MC, Carpita NC. 2015. Biomass recalcitrance: a multi-scale, multi-factor, and conversion-specific property. *J. Exp. Bot.* **66:** 4109-4118.

6. Zhang GC, Liu JJ, Kong II, Kwak S, Jin YS. 2015. Combining C6 and C5 sugar metabolism for enhancing microbial bioconversion. *Curr. Opin. Chem. Biol.* **29:** 49-57.

7. Guerriero G, Hausman JF, Strauss J, Ertan H, Siddiqui KS. 2016. Lignocellulosic biomass: biosynthesis, degradation, and industrial utilization. *Eng. Life Sci.* **16:** 1-16.

8. Rennie EA, Scheller HV. 2014. Xylan biosynthesis. *Curr. Opin. Biotechnol.* **26:** 100-107.

9. Numan MT, Bhosle NB. 2006. α-L-Arabinofuranosidases: the potential applications in biotechnology. *J. Ind. Microbiol. Biotechnol.* **33:** 247-260.

10. Poutanen K, Tenkanen M, Korte H, Puls J. 1991. Accessory enzymes involved in the hydrolysis of xylans, pp. 426-436. *In* Leatham GF, Himmel ME (eds.). *Enzymes in Biomass Conversion.* American Chemical Society, Washington, DC.

11. Dutta S, Wu KCW. 2014. Enzymatic breakdown of biomass: Enzyme active sites, immobilization, and biofuel production. *Green Chem.* **16:** 4615-4626.

12. Zheng HC, Sun MZ, Meng LC, Pei HS, Zhang XQ, Yan Z, *et al.* 2014. Purification and characterization of a thermostable xylanase from *Paenibacillus* sp. NF1 and its application in xylooligosaccharides production. *J. Microbiol. Biotechnol.* **24:** 489-496.

13. Lee SH, Lee YE. 2014. Cloning and characterization of a multidomain GH10 xylanase from *Paenibacillus* sp. DG-22. *J. Microbiol. Biotechnol.* **24:** 1525-1535.

14. Lee SH, Lee YE. 2014. Cloning, expression, and characterization of a thermostable GH51 alpha-L-arabinofuranosidase from *Paenibacillus* sp. DG-22. *J. Microbiol. Biotechnol.* **24:** 236-244.

15. Li F, Xie J, Zhang X, Zhao L. 2015. Improvement of the optimum pH of *Aspergillus niger* xylanase towards an alkaline pH by site-directed mutagenesis. *J. Microbiol. Biotechnol.* **25:** 11-17.

16. Werpy T, Peterson G. 2004. *Top Value Added Chemicals From Biomass.* Volume I—Results of Screening for Potential Candidates from Sugars and Synthesis Gas. Oak Ridge TN, US Department of Energy. Available at http://www.nrel.gov/docs/fy04osti/35523.pdf.

17. Chun BW, Dair B, Macuch PJ, Wiebe D, Porteneuve C, Jeknavorian A. 2006. The development of cement and concrete additive: based on xylonic acid derived via bioconversion of xylose. *Appl. Biochem. Biotechnol.* **131:** 645-658.

18. Zamora F, Bueno M, Molina I, Iribarren JI, Muñoz-Guerra S, Galbis JA. 2000. Stereoregular copolyamides derived from D-xylose and L-arabinose. *Macromolecules* **33:** 2030-2038.

19. Niu W, Molefe MN, Frost JW. 2003. Microbial synthesis of the energetic material precursor 1,2,4-butanetriol. *J. Am. Chem. Soc.* **125:** 12998-12999.

20. Sun L, Yang F, Sun H, Zhu T, Li X, Li Y, *et al.* 2016. Synthetic pathway optimization for improved 1,2,4-butanetriol production. *J. Ind. Microbiol. Biotechnol.* **43:** 67-78.

21. Bayer EA, Belaich J-P, Shoham Y, Lamed R. 2004. The cellulosomes: multienzyme machines for degradation of plant cell wall polysaccharides. *Annu. Rev. Microbiol.* **58:** 521-554.

22. Fontes CM, Gilbert HJ. 2010. Cellulosomes: highly efficient nanomachines designed to deconstruct plant cell wall complex carbohydrates. *Annu. Rev. Biochem.* **79:** 655-681.

23. Raman B, Pan C, Hurst GB, Rodriguez M Jr, McKeown CK, Lankford PK, *et al.* 2009. Impact of pretreated switchgrass and biomass carbohydrates on *Clostridium thermocellum* ATCC 27405 cellulosome composition: a quantitative proteomic analysis. *PLoS One* **4:** e5271.

24. Borne R, Bayer EA, Pagès S, Perret S, Fierobe HP. 2013. Unraveling enzyme discrimination during cellulosome assembly independent of cohesin-dockerin affinity. *FEBS J.* **280:** 5764-5779.

25. McClendon SD, Mao Z, Shin HD, Wagschal K, Chen RR. 2012. Designer xylanosomes: protein nanostructures for enhanced xylan hydrolysis. *Appl. Biochem. Biotechnol.* **167:** 395-411.

26. Morais S, Morag E, Barak Y, Goldman D, Hadar Y, Lamed R, *et al.* 2012. Deconstruction of lignocellulose into soluble sugars by native and designer cellulosomes. *MBio* **3:** e00508-e00512.

27. Liang Y, Si T, Ang EL, Zhao H. 2014. Engineered pentafunctional minicellulosome for simultaneous saccharification and ethanol fermentation in *Saccharomyces cerevisiae. Appl. Environ. Microbiol.* **80:** 6677-6684.

28. Ou J, Cao Y. 2014. Incorporation of *Nasutitermes takasagoensis* endoglucanase into cell surface-displayed minicellulosomes in *Pichia pastoris* X33. *J. Microbiol. Biotechnol.* **24:** 1178-1188.

29. Fan LH, Zhang ZJ, Yu XY, Xue YX, Tan TW. 2012. Self-surface assembly of cellulosomes with two miniscaffoldins on *Saccharomyces cerevisiae* for cellulosic ethanol production. *Proc. Natl. Acad. Sci. USA* **109:** 13260-13265.

30. Stern J, Morais S, Lamed R, Bayer EA. 2016. Adaptor scaffoldins: an original strategy for extended designer cellulosomes, inspired from nature. *MBio* **7:** e00083-e00016.

31. Wheeldon I, Minteer SD, Banta S, Barton SC, Atanassov P, Sigman M. 2016. Substrate channelling as an approach to cascade reactions. *Nat. Chem.* **8:** 299-309.

32. Mitsuzawa S, Kagawa H, Li Y, Chan SL, Paavola CD, Trent JD. 2009. The rosettazyme: a synthetic cellulosome. *J. Biotechnol.* **143:** 139-144.

33. Kagawa HK, Yaoi T, Brocchieri L, McMillan RA, Alton T, Trent JD. 2003. The composition, structure and stability of a group II chaperonin are temperature regulated in a hyperthermophilic archaeon. *Mol. Microbiol.* **48:** 143-156.

34. McMillan RA, Howard J, Zaluzec NJ, Kagawa HK, Mogul R, Li YF, *et al.* 2005. A self-assembling protein template for constrained synthesis and patterning of nanoparticle arrays. *J. Am. Chem. Soc.* **127:** 2800-2801.

35. McMillan RA, Paavola CD, Howard J, Chan SL, Zaluzec NJ, Trent JD. 2002. Ordered nanoparticle arrays formed on engineered chaperonin protein templates. *Nat. Mater.* **1:** 247-252.

36. Paavola CD, Chan SL, Li Y, Mazzarella KM, McMillan RA, Trent JD. 2006. A versatile platform for nanotechnology based on circular permutation of a chaperonin protein. *Nanotechnology* **17:** 1171-1176.

37. Mishra S, Beguin P, Aubert JP. 1991. Transcription of *Clostridium thermocellum* endoglucanase genes *celF* and *celD*. *J. Bacteriol.* **173:** 80-85.

38. Studier FW. 2005. Protein production by auto-induction in high density shaking cultures. *Protein Expr. Purif.* **41:** 207-234.

39. Lee CC, Kibblewhite-Accinelli RE, Smith MR, Wagschal K, Orts WJ, Wong DW. 2008. Cloning of *Bacillus licheniformis* xylanase gene and characterization of recombinant enzyme. *Curr. Microbiol.* **57:** 301-305.

40. Milner Y, Avigad G. 1967. A copper reagent for the determination of hexuronic acids and certain ketohexoses. *Carbohydr. Res.* **4:** 359-361.

41. Wagschal K, Franqui-Espiet D, Lee CC, Robertson GH, Wong DW. 2005. Enzyme-coupled assay for β-xylosidase hydrolysis of natural substrates. *Appl. Environ. Microbiol.* **71:** 5318-5323.

42. Wagschal K, Jordan DB, Lee CC, Younger A, Braker JD, Chan VJ. 2015. Biochemical characterization of uronate dehydrogenases from three pseudomonads, *Chromohalobacter salixigens*, and *Polaromonas naphthalenivorans*. *Enzyme Microb. Technol.* **69:** 62-68.

43. Lee CC, Smith M, Kibblewhite-Accinelli RE, Williams TG, Wagschal K, Robertson GH, Wong DW. 2006. Isolation and characterization of a cold-active xylanase enzyme from *Flavobacterium* sp. *Curr. Microbiol.* **52:** 112-116.

44. Pell G, Taylor EJ, Gloster TM, Turkenburg JP, Fontes CM, Ferreira LM, *et al.* 2004. The mechanisms by which family 10 glycoside hydrolases bind decorated substrates. *J. Biol. Chem.* **279:** 9597-9605.

45. Lee CC, Kibblewhite RE, Wagschal K, Li R, Orts WJ. 2012. Isolation of α-glucuronidase enzyme from a rumen metagenomic library. *Protein J.* **31:** 206-211.

46. Jordan DB. 2008. β-D-Xylosidase from *Selenomonas ruminantium*: catalyzed reactions with natural and artificial substrates. *Appl. Biochem. Biotechnol.* **146:** 137-149.

47. Stephens C, Christen B, Fuchs T, Sundaram V, Watanabe K, Jenal U. 2007. Genetic analysis of a novel pathway for D-xylose metabolism in *Caulobacter crescentus*. *J. Bacteriol.* **189:** 2181-2185.

48. Liu H, Valdehuesa KNG, Nisola GM, Ramos KRM, Chung WJ. 2012. High yield production of D-xylonic acid from D-xylose using engineered *Escherichia coli*. *Bioresour. Technol.* **115:** 244-248.

49. Toivari M, Nygård Y, Kumpula EP, Vehkomäki ML, Benčina M, Valkonen M, *et al.* 2012. Metabolic engineering of *Saccharomyces cerevisiae* for bioconversion of D-xylose to D-xylonate. *Metab. Eng.* **14:** 427-436.